

RADAR SENSING OF ULTRA-HIGH ENERGY COSMIC RAY SHOWERS

by

Jon Paul Lundquist

A Senior Honors Thesis Submitted to the Faculty of
the University of Utah
in Partial Fulfillment of the Requirements for the

Honors Degree of Bachelor of Science

in

Physics

APPROVED:

John Belz
Supervisor

David Kieda
Chair, Physics

John DeFord
Departmental Honors Advisor

Martha S. Bradley
Dean, Honors College

December 15, 2009

ABSTRACT

The intent of this paper is to review the history and potential importance of the use of radar techniques in detecting the ionization columns of ultra-high energy cosmic ray showers and give a short overview of a currently planned radar experiment at the Telescope Array. There is much activity in cosmic ray research to study the composition and source locations of this phenomena. Radar would be an important addition to fluorescence and scintillation detection as it theoretically could attain greater volume coverage and nearly the accuracy of fluorescence systems with less infrastructure and much longer running times. The currently estimated mean echo lifetime is on the order of $50 \mu\text{s}$ for a cosmic ray of energy 10^{19} eV. It is shown that a continuous wave bi-directional radar system transmitting in the low-VHF with a large obstruction between receiver and transmitter (such as a mountain or earth curvature), which assures direct transmission is reduced, is the nominal configuration and the planned radar experiment at the Telescope Array satisfies these requirements.

TABLE OF CONTENTS

Abstract	ii
1 Introduction	1
2 Characterization of Ionization Columns	3
3 Signal Duration	8
4 Signal to Noise Ratio	12
5 Radar Experiment at Telescope Array	15
6 Conclusion	25
A AREPS Instruction	30

Chapter 1

Introduction

Ultra-high energy cosmic rays (UHECR's) are those particles which are just below or exceed the theoretical GZK[1][2] cutoff limit of 5×10^{19} eV. This limit is imposed by the cosmic background radiation interacting with the cosmic ray particle. A number UHECR's have been detected over a number of years. One of the highest energy cosmic rays recorded was 3.2×10^{20} eV[3].

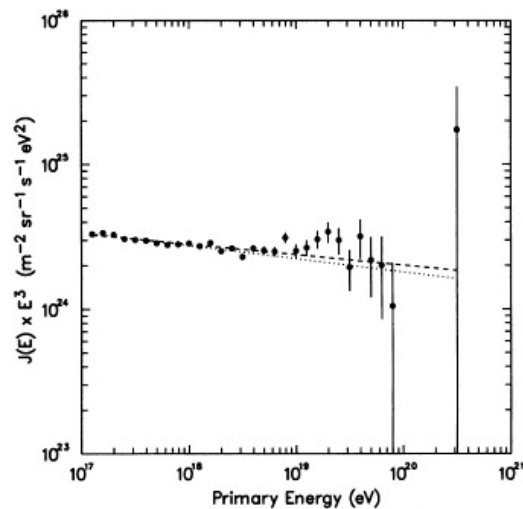


FIG. 11.—Fly's Eye monocular energy spectrum. *Points*: data. *Dashed line*: best fit of the total spectrum. *Dotted line*: best fit up to $10^{19.5}$ eV.

Figure 1.1: Fly's Eye Experiment energy spectrum showing particle of 3.2×10^{20} eV[3]

To put this in perspective the highest proton collision energy to be achieved by the Large Hadron Collider (LHC) is 1.4×10^{13} eV[4]. That is 22.9 million times less energetic and is only for protons; cosmic ray primary particles consist of electrons, protons, alpha particles, all the way up to iron nuclei. When these particles hit the atmosphere they create extensive air showers (EAS) through secondary interactions which start when they collide with an atmospheric nucleus. These showers propagate at the nearly the speed of light and increase in size until they reach a maximum. This creates a column of ionized air behind a relativistic disk of particle interactions that can be detected using radar techniques that have been used to study meteors for many years.[5][6][7]

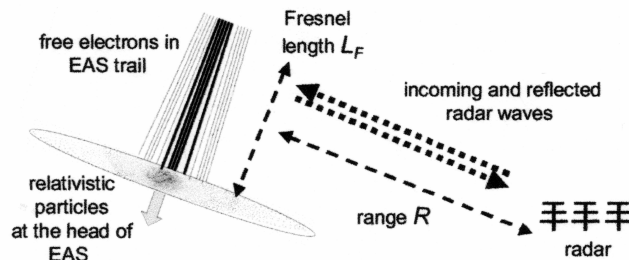


Fig. 1: The geometry for a specularly reflected radar echo by free electrons produced in the trail region of an EAS.

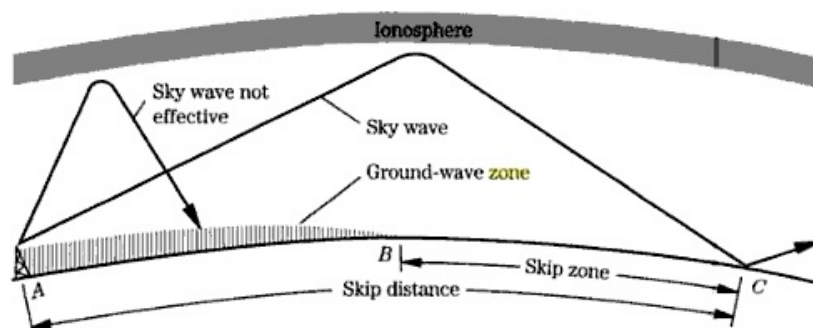
Figure 1.2: Diagram of EAS shower and ionization column[8]

Cosmic rays of this energy are extremely rare therefore it is of great interest to be able to collect as much data as possible on this phenomena. UHECR's have implications for dark matter[9], possible standard model modifications, the intergalactic medium, space travel, even genetic evolution[10]. It will be shown that radar detection of UHECR's has the capability to increase the detection volume and running time over fluorescence detectors.

Chapter 2

Characterization of Ionization Columns

In the late 1930's many radio reflections were detected[11][12][13][14] that occurred in what is called the "skip zone" at altitudes of 10 to 150 km high where they should not have been detected under normal circumstances. These signals were thought to be caused by some kind of intermittent reflective ionization clouds. Suggestions for the cause of these signals were "solar activity, aurora phenomena, thunderstorms, meteorites and water vapour discontinuities." [15]



2-31 Relationship between ground wave and different cases of sky wave.

Figure 2.1: Diagram of the Ionosphere Skip Zone and Ground-wave Zone[16]

In 1940 Blackett and Lovell were the first to suggest that at least some of this anomalous radio scattering could be explained by the ionization from extensive cosmic ray air showers.[15] It was later shown that the signals at higher altitudes were actually caused by meteors. This dampened interest in radar sensing of EAS for many years.[5] This demonstrates the need to differentiate the differences between UHECR EAS ionization columns and other types of events.

This was done in P. Gorham's extensive treatment of radar detection of cosmic rays[5] and what follows is a paraphrase of that paper. Radar detected meteors generally occur at a height of 80-120 km which is also the height of lower energy cosmic rays that are not of interest. In meteors there is an initial radius of 2-10 m and the radial ionization density is nearly uniform. The ionization column is eventually dissipated by electron attachment and recombination. The fastest meteors travel at approximately 100 km/s and after the meteor is depleted of material radar echoes for frequencies from 10-100 MHz can be detectable for several seconds.[5]

Lightning ionization column charge densities are orders of magnitude higher than either meteors or EAS and have a much smaller diameter. Therefore their radar echoes should be longer than for EAS. They do sometimes occur in clusters transverse to the earth at EAS maximum particle volume, X_{max} , altitudes.[5] The X_{max} altitude is on average roughly 10 km for UHECR's.[5][17]

EAS ionization columns on the other hand have a distribution that spreads out radially as the length increases and propagates at nearly the speed of light. This radial distribution of ionization is much more complicated than the meteor case. 90% of the charged particles can be found within what is called the Moliere radius r_m (about 70 m at sea level) and the distribution within this radius follows a power law. This means that a significant amount (10%) of the ionization can be found within less than 1% of the area of the Moliere radius or about 3.5 meters at sea level.[5] The electron density near the core can reach above $n_e = 10^{14} m^{-3}$ [6]

Blackett and Lovell[15] used a point cluster approximation where the effective

number of ions is that of a column the length of the first Fresnel zone which is dependent upon the wavelength of the incident radar. This length is[5]

$$L = \sqrt{\frac{\lambda R}{2}} \quad (2.1)$$

R is the distance from the shower to transmitter. They estimated that the maximum number of effective electrons per centimeter of air multiplied by L (or the total number of effective electrons), where p is the fraction of 1 atm at the height of the shower and E is the incident electron energy, is

$$N_e = \frac{1}{2} 10^{-7} \text{ cm}^{-1} p E \sqrt{\lambda R} \quad (2.2)$$

The most important factor in characterizing the effective ionization column is the relationship between the plasma frequency ν_p and the radar frequency.[5]

$$\nu_p = \sqrt{\frac{n_e e^2}{4\pi^2 \epsilon_0 m_e}} \simeq 8.98 \times 10^3 \text{ m}^{3/2} \sqrt{n_e} \text{ Hz} \quad (2.3)$$

This is used to divide the ionization columns into two categories called overdense and underdense ionization columns. If the electron density is high enough that $\nu_p > \lambda$ it falls in the overdense case and the reflections will be specular or mirror-like. If $\nu_p < \lambda$ it falls in the underdense case and the radar is able to penetrate the ionization column. In this case the reflections are caused by coherent electron scattering and the return power will depend quadratically on electron density. This would possibly allow radar estimates of the energy of the primary particle by determination of the EAS electron density. [5]

The effective radar cross section (RCS) for the overdense case can be approximated as a metal cylinder with a radius r_c at the point the ionization column becomes overdense. This is where the RCS is the greatest. The case when r_c is much greater than the radar wavelength (Optical regime) is only relevant for very high shower

energies and very low radar frequencies and is not important. In the subcategory where r_c is much less than the radar wavelength (Rayleigh regime) the RCS can be approximated as a thin wire.[5] This approximation is

$$\sigma_{b,\text{maz}}^{\text{od}} \simeq \frac{\lambda^2 \tan^2 \theta \cos^4 \phi}{16\pi \left[\left(\frac{\pi}{2}\right)^2 + (\ln [\lambda / (1.78\pi r_c \sin \theta)])^2 \right]} \quad (2.4)$$

The angle ϕ is the angle of linear polarization with respect to the axis of the wire and θ is the zenith angle measured from the wire axis. Unfortunately, using a frequency below 10 MHz which is required for this case would be sensitive to geometric effects which make determination of the ionization amount difficult. It is possible that this was responsible for the anomalous skip zone detections mentioned by Blackett and Lovell.[7] Therefore, the underdense case is the best scenario to aim for. This means using higher frequency radar.

Only when the radar frequency is less than 10 MHz will the underdense case, where r_m , the Moliere radius previously mentioned, is much less than the radar wavelength (Rayleigh regime), be encountered. That leaves the most important case where $r_m \geq \lambda/4$ and the radar frequency is greater than the plasma frequency. This is called the optical regime. In this case there is no longer coherent scattering and the electron phase factors must be taken into account.[5] For a monostatic radar system, where the transmitter and receiver are located in the same place, the RCS becomes

$$\sigma_b^{\text{ud}}(\mathbf{q}) = \sigma_T \left| \int n_e(\mathbf{r}) e^{i\mathbf{q} \cdot \mathbf{r}} d^3\mathbf{r} \right|^2 \quad (2.5)$$

Where σ_T is the Thomson cross section,

$$\sigma_T = \frac{8\pi}{3} \left(\frac{e^2}{m_e c^2} \right)^2 = 6.65 \times 10^{-29} m^2 \quad (2.6)$$

$\mathbf{q}=2*\mathbf{k}$ and \mathbf{k} is the wave vector of the incident radio wave and \mathbf{r} is the vector distance to the scattering volume element. [5]

The ionization density pattern can be further characterized using the NKG approximation[18][19] to find the RCS. The conclusion is that ionization density is highly concentrated within .5 m at 10 km for horizontal showers and for total reflection the highest radar frequencies are 10-50MHz.[5]

The underdense optical regime, which again is the most important for the ionization columns of UHECR EAS, can be parameterized in the case of a horizontal EAS by [5]

$$\sigma_b^{\text{ud}}(10 \text{ km}) = 175 \left(\frac{f}{30 \text{ MHz}} \right)^{-1.84} \left(\frac{E}{10^{20} \text{ eV}} \right)^{1.9} \left(\frac{R}{10 \text{ km}} \right) m^2 \quad (2.7)$$

$$\sigma_b^{\text{ud}}(5 \text{ km}) = 1400 \left(\frac{f}{30 \text{ MHz}} \right)^{-1.15} \left(\frac{E}{10^{20} \text{ eV}} \right)^{1.9} \left(\frac{R}{10 \text{ km}} \right) m^2 \quad (2.8)$$

For normal incidence and oblique angles from 60° to 120° the radar cross section is graphed for frequencies from 10 to 50 MHz for a UHECR of $E = 10^{20} \text{ eV}$

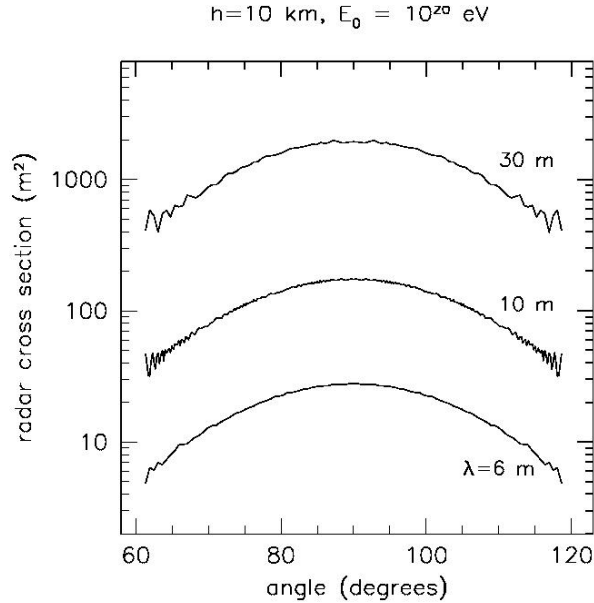


Figure 2.2: Range of RCS at 10 km for a cosmic ray of $E= 10^{20} \text{ eV}$ [5]

Chapter 3

Signal Duration

The exact echo signal duration for EAS ionization columns, to this date, appears to be controversial. Ionization column duration must be long enough for a standalone system pulsing on a set frequency, or a radar system triggered by a fluorescence or scintillator detector, to reflect a signal off of it. If the ionization column lifetime is too short then a pulse system will not work and a continuous wave system would have to be considered.[5][6]

In 1940 Blackett and Lovell stated that the signal duration is the lifetime of free electronic ions. This is dependent on the rate of molecule attachment and is "roughly inversely proportional to the pressure, and will have a value of 10^{-5} to 10^{-6} sec at ground level and of the order of a second at 100 km." Also, the amplitude times the duration is constant, so the higher the cosmic ray the less amplitude the echo will have.[15] The conclusion is that the signal duration would be on the order of $t = .1$ sec at 10 km.

In 1968 T. Matano, et al [20] stated that the collision mean time of electrons is about 10^{-9} sec, the electron mean lifetime is about 10^{-7} sec, and the recombination of positive and negative ions is several minutes. It was intended that to increase the received echo power 10^4 radar pulses would be reflected from the EAS column in the several minutes before recombination completes and the entire RCS dissipates.

In 2001 P. W. Gorham[5] considered diffusion, attachment, and recombination effects on pulse duration. It is also shown that radar frequency affects the signal duration. If diffusion processes on EAS are the same as meteor ionization columns then the time constant, the time in which the decay becomes exponential, would be approximately 60 sec for a frequency of 100 MHz for EAS. But lightning columns which have a higher density than either meteor or EAS column have a time constant of around 240 ms which suggests that other processes are more important than diffusion. The time constant for attachment gives an even larger value of several minutes for high energy EAS. This leaves recombination as the deciding factor in echo signal duration. The conclusion is that the signal duration at an altitude of 10 km is bounded by

$$20\mu s \leq \tau_e \leq 20ms \quad (3.1)$$

This would mean that triggered detection is not possible for the lowest lifetimes unless the EAS is within a few kilometers. For the longest lived columns triggered detection from more than 1000 km would be possible.[5]

In Gorham's next paper that same year it is stated that the previous estimate depended on a 2-body attachment process and that it is likely by the time the paper is published that it will be found that 3-body attachment is the dominant process.[7] This would reduce the echo lifetime to roughly .1 μs . A continuous wave radar system would be needed as no pulsed radar would be sufficient for such a short time frame.

The lifetime can also be decreased in moist air, therefore higher altitude shower echo pulses would be less affected by moisture.[7] This also means that a radar system located in a dry climate is preferable.

In the same year as Gorham's papers T. Vinogradova, et al state that the ionization column is 10-20 km long and is highly reflective for frequencies below 100 MHz on a timescale of the order of 100 μs . [17]

More recently H. Takai states that signal duration depends heavily on the ori-

entation of the ionization column. Only a part of the EAS will be scattering radio waves at any given time and the total signal time is the integration over these segments. The shortest and longest signals are those moving towards or away from the receiver. The figure 5 shows these cases as a function of inclination angle α for the two extreme cases of the azimuthal angle β measured at the EAS tail with respect to the transmitter. The conclusion is the signals would be between about 1 to 68 μs [6]

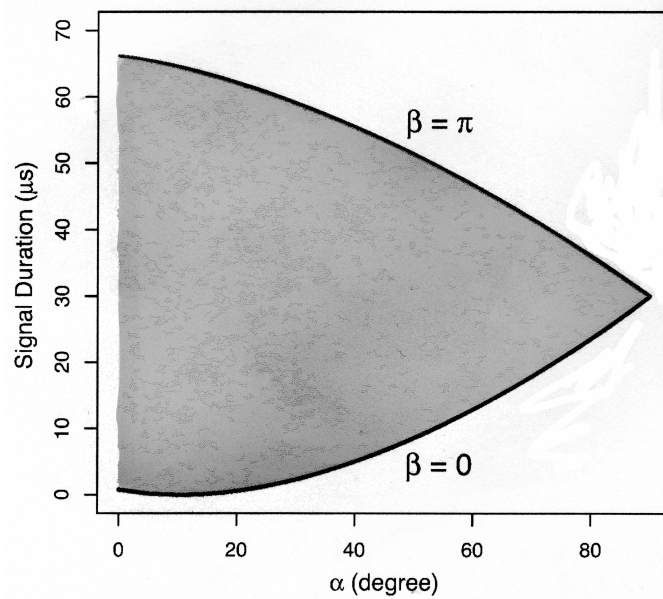


Fig. 5. Schematic view for the scattering

Figure 3.1: Range of signal durations between two extreme cases[6]

This year T. Terasawa, et al, stated that EAS echo duration should be on the order of $L/c + t_e$. Where L is the Fresnel length and t_e is the lifetime of free electrons. They state that Gorham's estimation is far too long and should likely be several μs or shorter.[8] Their estimate is roughly 2 to 4 μs based on the t_e value given by R. J. Vidmar in 1990.[21]

What can be seen from this discussion is that the important factor is the mean electron lifetime and the length of the ionization column. Signal duration will also be

dependent on shower direction, angle, and air moisture. It is clear that at this time a radar experiment would need to find coincidences between echo signals and detected events from a more proven method such as fluorescence or scintillator detectors for a conclusive statement about signal lifetimes. Taking out the outliers and averaging they will likely be roughly on the order of $50 \mu s$.

Chapter 4

Signal to Noise Ratio

For a monostatic system, where the antenna is at the same position as the transmitter, P. Gorham[7] calculated the signal-to-noise ratio (SNR) to be

$$\frac{P_r}{P_N} = \sigma_b P_t \eta \frac{G^2 \lambda^2}{(4\pi)^3 R^4} \frac{1}{k T_{sys} \Delta f} \quad (4.1)$$

The radar return power is P_r , P_t is the peak transmitted power, and the directivity gain is G , σ_b is the effective radar backscatter cross-section given earlier, R is the range, and lastly η is the efficiency of the transmitter-receiver system.[7] The noise power is given by

$$P_n = k T_{sys} \Delta f \quad (4.2)$$

where k is the Boltzmann constant, Δf is the receivers effective bandwidth, and T_{sys} is the system noise temperature. If echo signal durations are long enough, multiple pulses can be averaged to increase the SNR. The ratio can be multiplied by approximately \sqrt{N} which is the square root of the number of pulses used to interrogate the EAS.[7] The signal to noise ratio can be optimized by using the lowest radar frequency that is possible taking into consideration background noise while also staying within the underdense regime. Just over 50 MHz is nominal in a remote area

where the system temperature when given by

$$T_{\text{sys}} = 2.9 \times 10^6 \left(\frac{f}{3\text{MHz}} \right)^{-2.9} K \quad (4.3)$$

is 621 K for 55.25 MHz. Parameterizing equation 4.1 gives

$$\frac{S}{N} = 3.3 \left(\frac{\sigma_b}{1m^2} \right) \left(\frac{P_t}{1kW} \right) \left(\frac{\eta}{0.1} \right) \left(\frac{G}{10} \right)^2 \left(\frac{\lambda}{3m} \right)^2 \left(\frac{R}{10^4m} \right)^{-4} \left(\frac{T_{\text{sys}}}{10^3K} \right)^{-1} \left(\frac{\Delta t}{10\mu s} \right) \quad (4.4)$$

where Δt is the transmitted pulse duration.[7]

According to H. Takai [6] for a bi-static radar system, where the antenna is at the other side of the EAS from the transmitter, while taking into account that only a part of the EAS is reflecting radio waves at a given time, and that therefore the SNR will depend upon EAS orientation, the received power P_r can be written as

$$dA = A_0(s)\kappa(h) \sin \left[\omega \left(t - \frac{R_R}{c} \right) - \phi(R_T, R_R) \right] q_0(s) e^{-(t - \frac{R_R}{c})/\tau(h)} H(s) ds \quad (4.5)$$

for Thomson scattering at each shower segment. $\kappa(h)$ is thermalization attenuation, $\tau(h)$ is the free electron lifetime, h is altitude, $\phi(R_T, R_R)$ is the phase of the wave at the receiving antenna and $H(s)$ is the Heaviside function indicating that the segment radiates only when created. $A(s)$ is the scattering amplitude for each segment and is similar to the first half of equation 4.1 but is for the bi-static case and is separated into components of transmitter and receiver.[6]

$$A(s) = \left(2Z_{\text{in}} \frac{P_T G_T}{4\pi R_T^2} \frac{\sigma_e}{4\pi R_R^2} G_R \frac{\lambda^2}{4\pi} \right)^{1/2} \quad (4.6)$$

Z_{in} is the "electron cloud power density"[6] and σ_e is the single electron scattering cross section given in equation 4.7. r_e^2 is the classical electron radius and γ is "the

angle between the electric field of the incoming wave at the scattering center and the vector that connects to R.”[6]

$$\sigma_e = 4\pi r_e^2 \sin^2 \gamma \quad (4.7)$$

A graph is given of the dependence on azimuthal angle for a receiver 100 km from a 50 kW transmitter and a shower of $E=10^{19}$. Four different inclinations are shown. Both antenna have $G = 10$ in this case.[6]

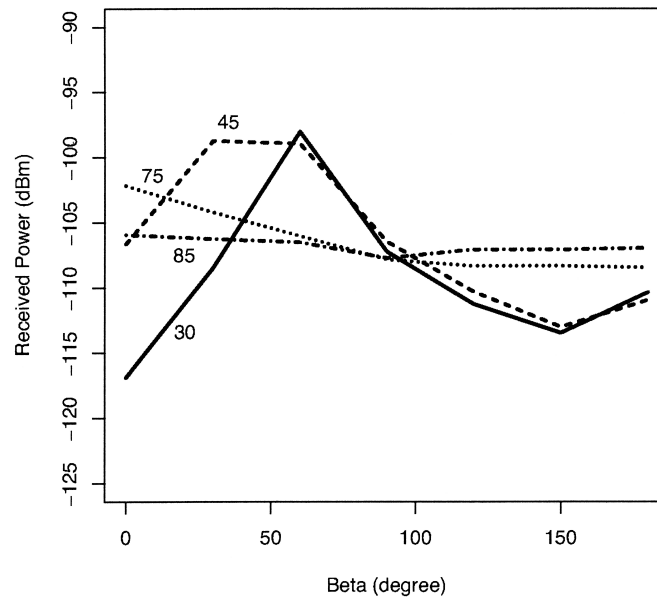


Figure 4.1: Received power dependence on azimuthal angle of a shower of $E=10^{19}$ for four different inclinations.[6]

Chapter 5

Radar Experiment at Telescope Array

A directional dipole transmitter will be placed at the Cosmic Ray Center(CRC) which is located in Delta, Utah at $39^{\circ}21'10.7''\text{N}$ $112^{\circ} 35'22.34''\text{W}$. Receiving antennae will be placed in the area of the Telescope Array Longridge facility(LR) which is at $39^{\circ}21'28.44''\text{N}$ $113^{\circ} 07'17.29''\text{W}$. From the CRC the LR facility is 250.5° from north and the distance between them is roughly 45 km. See Figure 5.1. The transmitting antenna to be used has a gain of $G=7.5$ and will be run at a transmission power of $P_t=2$ kW at the frequency $f = 55.25$ MHz ($\lambda = 5.43$ m)[22]

From the CRC the center of the Telescope Array(TA) is roughly 25 km away and the maximum particle volume altitude X_{max} for showers of $E = 10^{20}$ eV is just below 3000 m above ground. Ground level is just above 1400 m within the TA area. This means that for the following calculations $X_{max} = 4400$ m, $R = \sqrt{(25\text{km})^2 + (3\text{km})^2} \simeq 25\text{km}$ for the 5 km parameterization (Equation 2.8), and $R= 27$ km for 10 km (Equation 2.7).

The Fresnel length is,

$$L = \sqrt{\frac{5.43 \text{ m } 25 \times 10^3 \text{ m}}{2}} = 261 \text{ m} \quad (5.1)$$

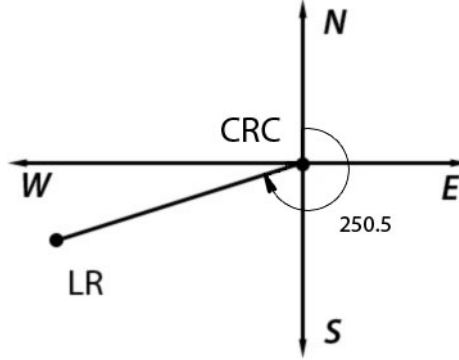


Figure 5.1: Diagram of angle from north of the LR facility at the CRC.

Where $p=.513$ at 4400 m[24] the total number of effective electrons is (Equation 2.2),

$$N_e = \frac{1}{2} 10^{-7} \text{ cm}^{-1} \cdot .513 \cdot 10^{20} \cdot 261 \text{ m} = 7 \times 10^{16} \quad (5.2)$$

The Moliere radius is[25],

$$r_m = 74 \left(\frac{p_o}{p} \right) m = 144 \text{ m} \quad (5.3)$$

Therefore, the electron density at the radius which comprises 1% of the area of the disc and within which 10% of the electrons are located, is,

$$n_e = \frac{.1 \cdot 7 \times 10^{16}}{\pi \left(\frac{144 \text{ m}}{20} \right)^2 261 \text{ m}} = 1.6 \times 10^{13} \text{ m}^{-3} = 1.6 \times 10^5 \text{ cm}^{-3} \quad (5.4)$$

Then the plasma frequency v_p is (Equation 2.3),

$$v_p = 8.98 \times 10^3 \text{ m}^{3/2} \sqrt{1.6 \times 10^5 \text{ cm}^{-3}} \text{ Hz} = 3.6 \text{ MHz} \quad (5.5)$$

This ensures that a radar of frequency of 55.25 MHz will completely penetrate a shower of $E = 10^{20}$ eV over TA. This situation is squarely in the underdense optical

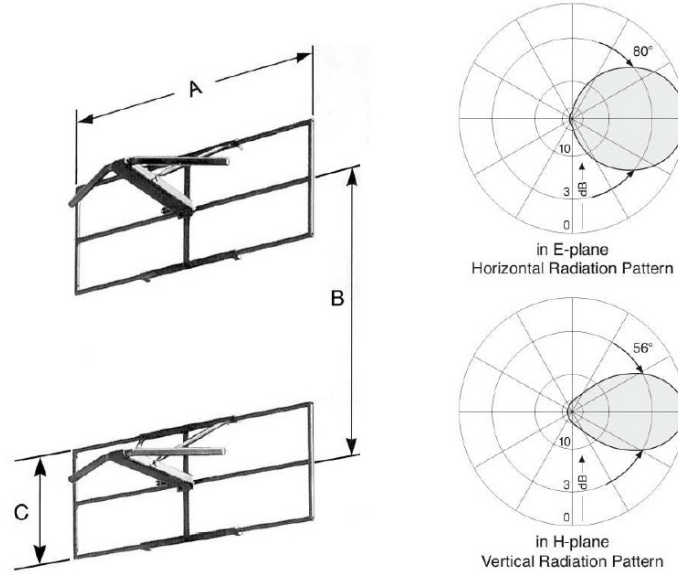


Figure 5.2: Transmitting antenna and antenna radiation pattern.[23]

case because $r_m \geq \lambda/4$ and $f > v_p$.

Referring to equations 2.7 and 2.8 the results for the radar cross section at altitudes of 4.4 and 10 km are,

$$\sigma_b^{\text{ud}}(5 \text{ km}) = 1400 \left(\frac{55.25 \text{ MHz}}{30 \text{ MHz}} \right)^{-1.15} \left(\frac{10^{20} \text{ eV}}{10^{20} \text{ eV}} \right)^{1.9} \left(\frac{25 \text{ km}}{10 \text{ km}} \right) m^2 = 1734 m^2 \quad (5.6)$$

$$\sigma_b^{\text{ud}}(10 \text{ km}) = 175 \left(\frac{55.25 \text{ MHz}}{30 \text{ MHz}} \right)^{-1.84} \left(\frac{10^{20} \text{ eV}}{10^{20} \text{ eV}} \right)^{1.9} \left(\frac{27 \text{ km}}{10 \text{ km}} \right) m^2 = 154 m^2 \quad (5.7)$$

For a monostatic configuration we can use equation 4.4 to find the estimated signal to noise ratio. This can also be considered bi-static from the center of TA only if the receiver and transmitter happen to have the same gain and system noise. The system noise is estimated based on the noise spectrum recorded at the CRC using a

6-element Yagi antenna.[22]

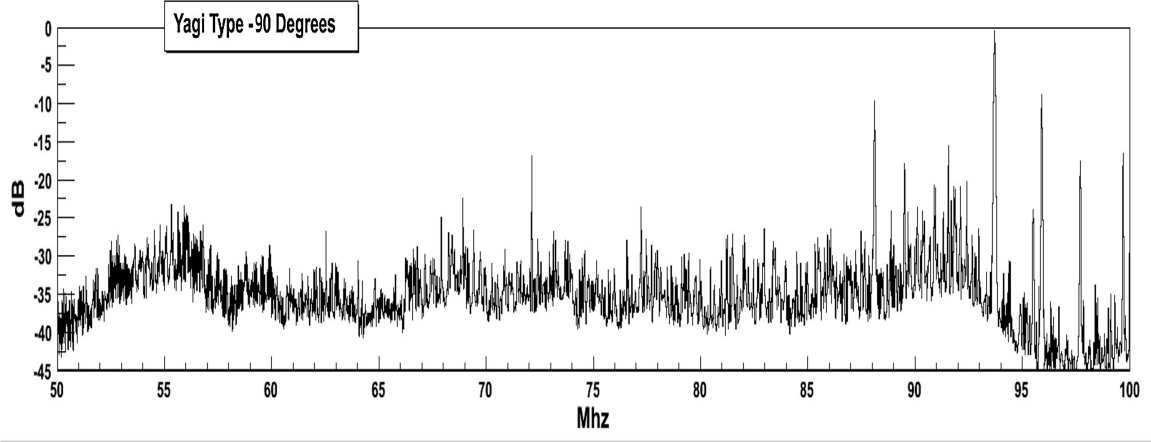


Figure 5.3: Noise spectrum recorded at the CRC using a 6-element Yagi antenna.[22]

The system temperature for $f = 55.25$ MHz is given by[26],

$$T_{\text{sys}} = 290 \cdot (10^{\log(\text{NoiseFactor})} - 1) = 290 \cdot (10^{1\log(30)} - 1) = 8410K \quad (5.8)$$

This value is greater than that estimated by equation 4.3.

For a horizontal EAS at 4400 m,

$$\frac{S}{N} = 3.3 \left(\frac{1734m^2}{1m^2} \right) \left(\frac{2 \text{ kW}}{1 \text{ kW}} \right) \left(\frac{0.1}{0.1} \right) \left(\frac{7.5}{10} \right)^2 \left(\frac{5.43m}{3m} \right)^2 \left(\frac{25km}{10^4m} \right)^{-4} \left(\frac{8410K}{10^3K} \right)^{-1} = 64.20 \quad (5.9)$$

For a horizontal EAS at 10 km,

$$\frac{S}{N} = 5.26 \quad (5.10)$$

These values are far more than sufficient to see a signal from such a UHECR EAS. For a bistatic case the gains and system temperatures will be different. Also the system efficiency will likely be less than .1 and most EAS will not be exactly horizontal

right in the middle of TA. Therefore these values can be considered maximums and the real ratios will be less.

To minimize direct transmission from transmitter to receiver the receivers will be placed behind an obstruction. A simulation was done using the Advanced Refractive Effects Prediction System (AREPS)[27] made by the U.S. Navy which shows the signal attenuation as it travels over the Telescope Array. AREPS uses the Advanced Propagation Model which is a hybrid ray-optic and parabolic equation model. Figure 5.4 shows the areas that AREPS uses these different models.

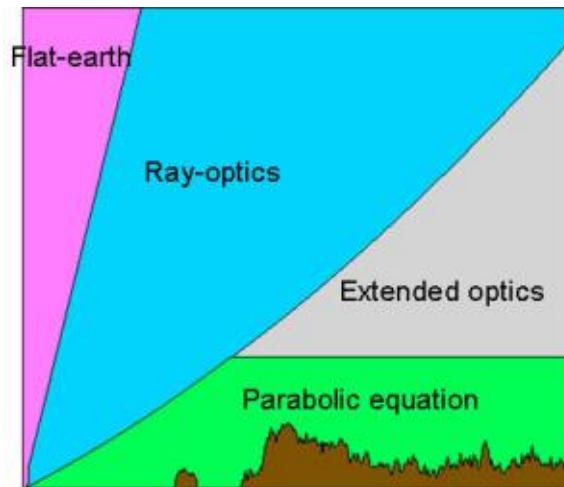


Figure 5.4: Advanced Propagation Model component diagram. Bottom left is the transmitter location and the brown area is ground.[27]

In the following figure 5.5 the transmitter attenuation is shown for the transmitter at a great height using the verticle antenna pattern. No ground information is included to demonstrate atmospheric effects.

In the next set of figures ground information is added and the transmitter is moved closer to the ground to show ground effects.

The final diagram (Figure 5.9) is with the transmitter at the likely elevation of 50 ft above ground. In this configuration the transmitter power is relatively uniform

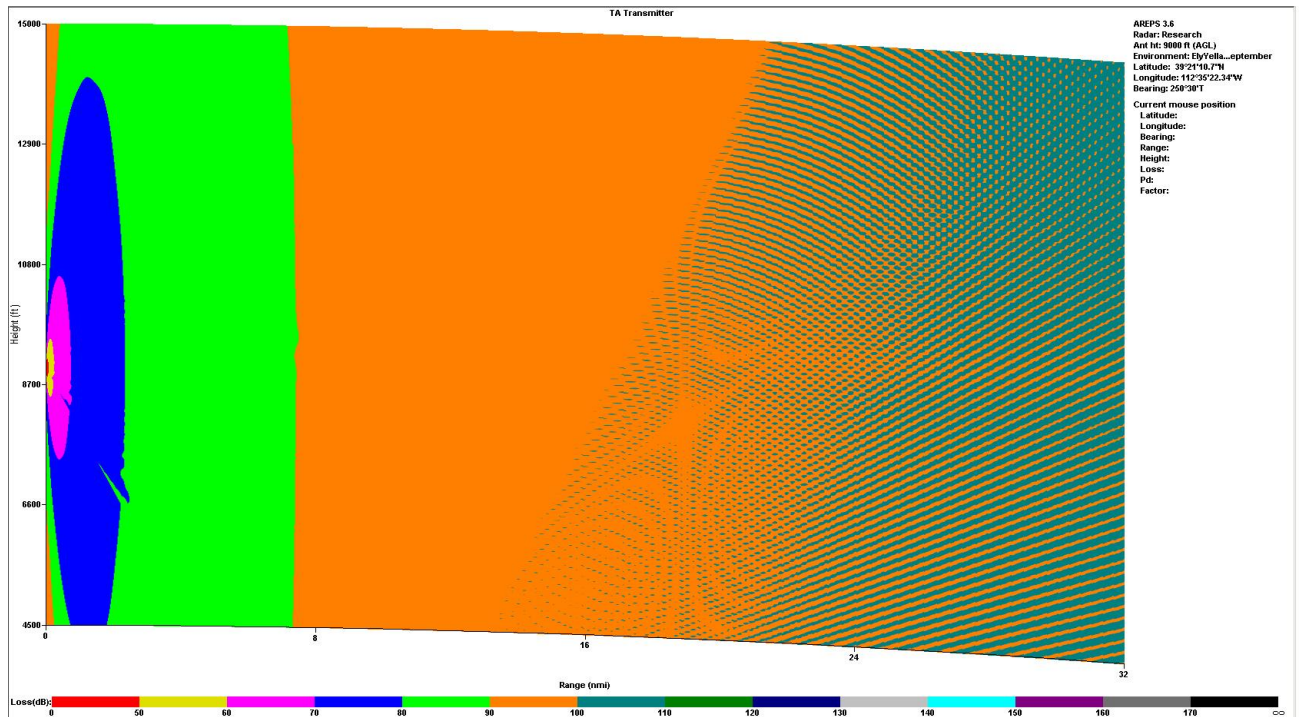


Figure 5.5: Transmitter attenuation in db over TA with no ground information included. Each color change is a loss of 10db.

directly over TA at X_{max} with a loss of 90 to 100 db from the original signal. The received signal at Longridge on the other hand will have an estimated power loss of about 155 db. This means that the EAS probing signal strength will be a factor of 10^6 more powerful than the direct signal received which ensures that the direct signal should be well below the noise floor. This should be an excellent system configuration.

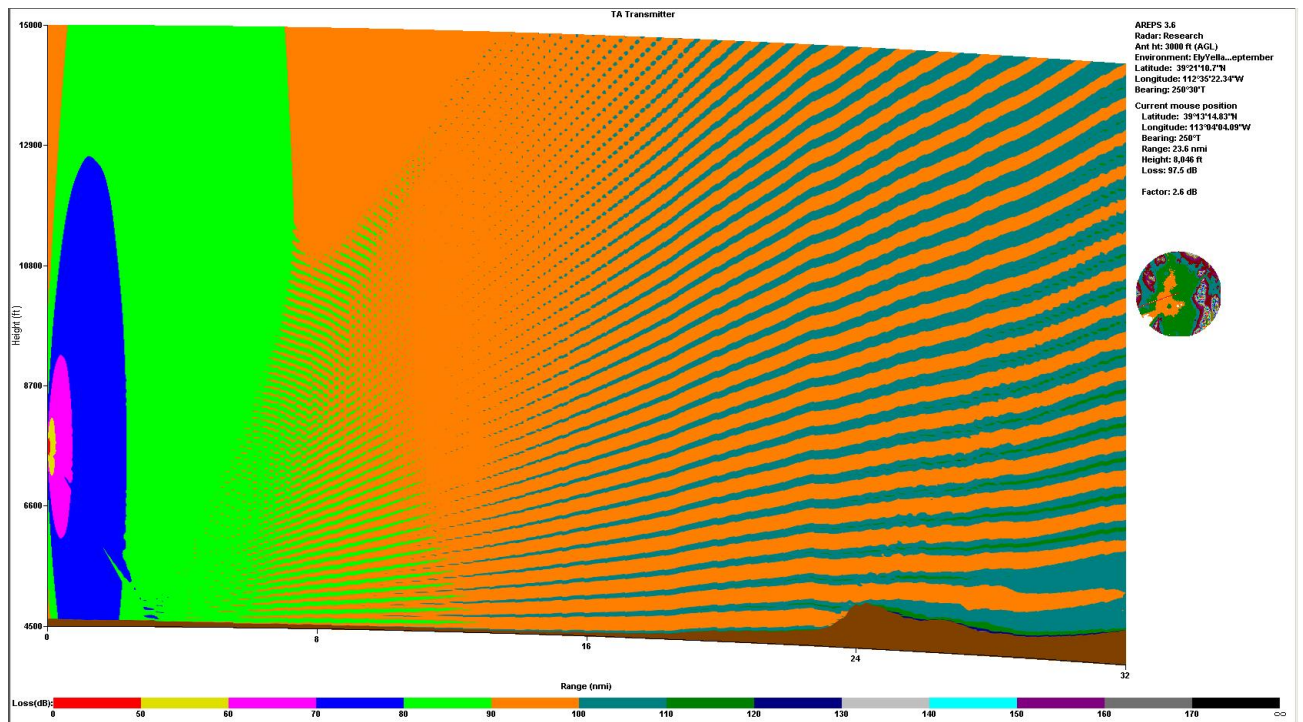


Figure 5.6: Transmitter attenuation in db over TA with ground information included. Transmitter elevation of 7650 ft.

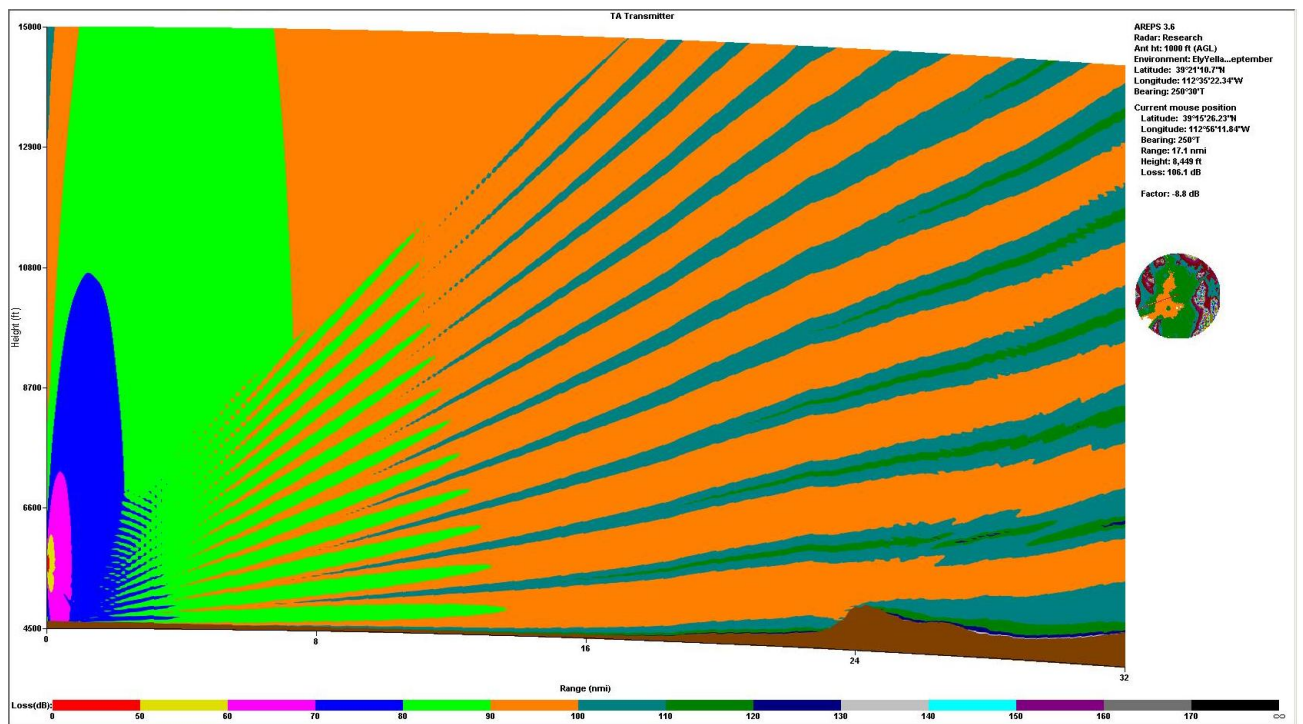


Figure 5.7: Transmitter attenuation in db over TA with ground information included. Transmitter elevation of 5550 ft.

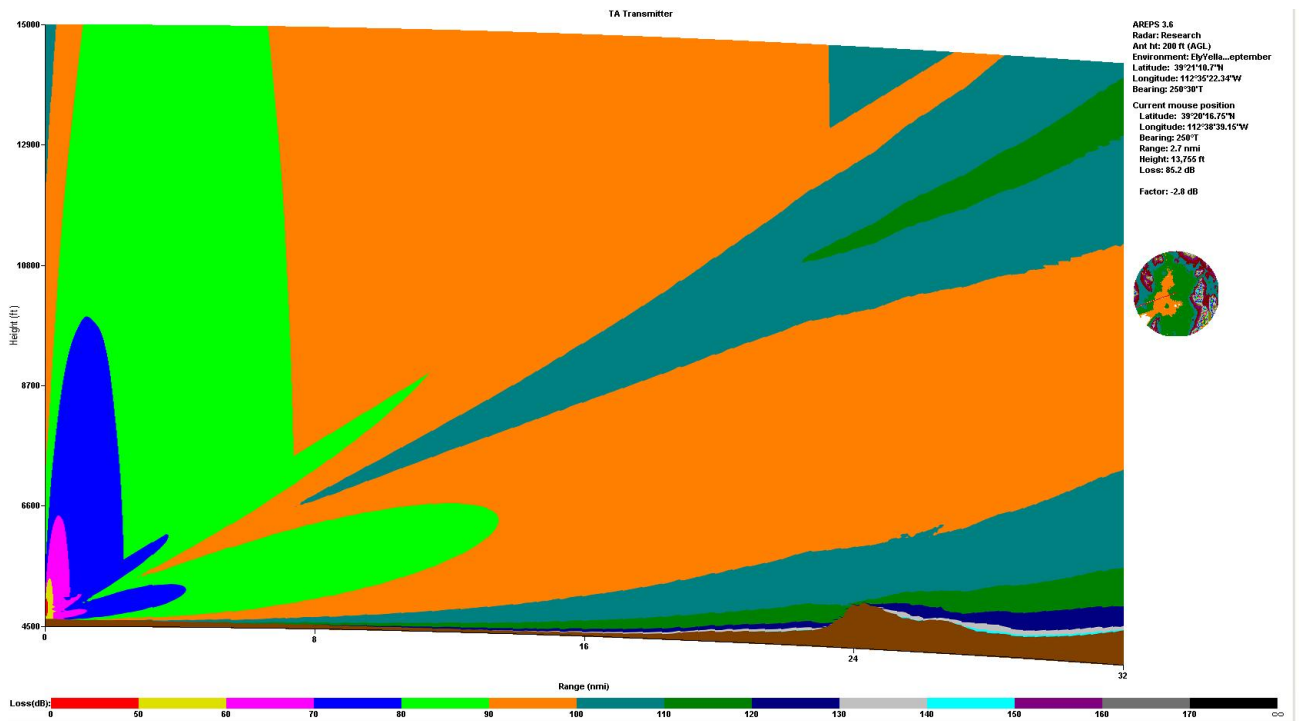


Figure 5.8: Transmitter attenuation in db over TA with ground information included. Transmitter elevation of 200 ft above ground.

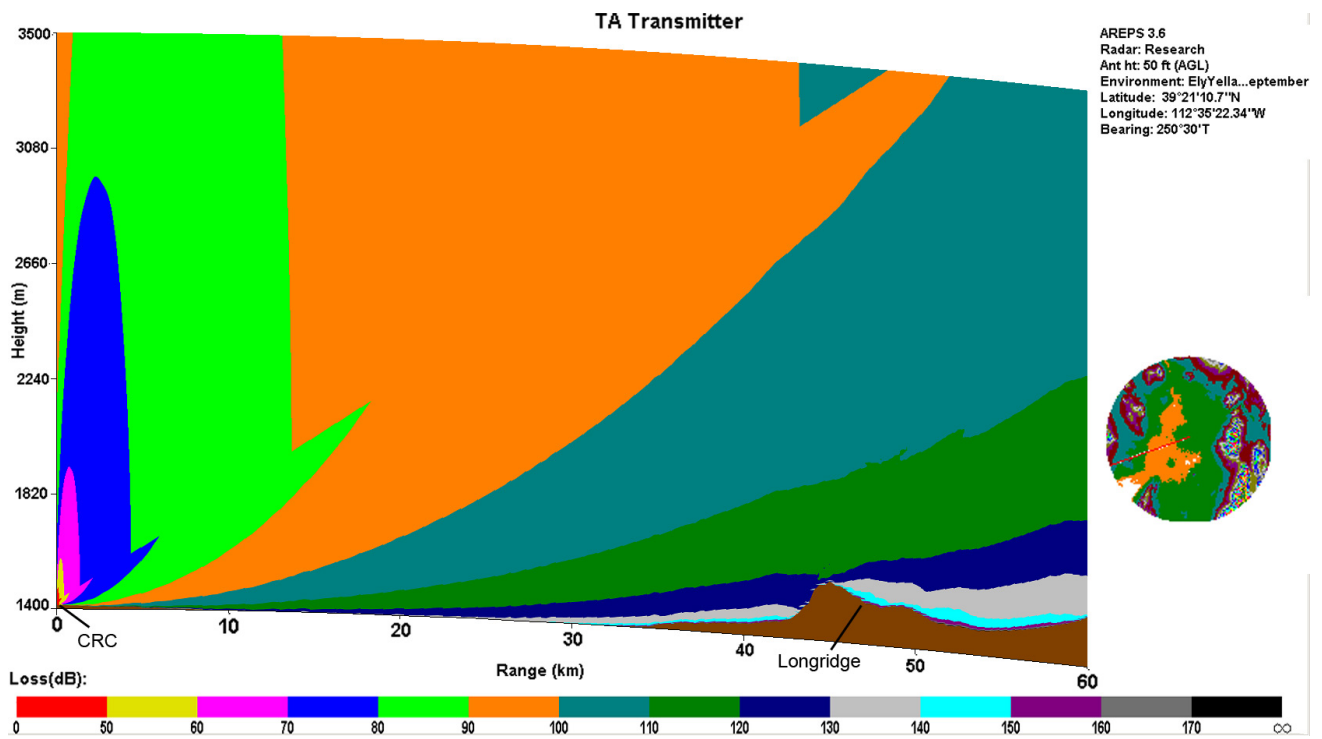


Figure 5.9: Transmitter attenuation in db over TA. Transmitter elevation of 50 ft above ground.

Chapter 6

Conclusion

Because the radar echo lifetime is as yet unknown it may be too short for pulsed radar, thus a continuous wave radar system should be run in conjunction with a fluorescence or scintillation detection system. To maximize echo lifetimes a dry location would be needed. A bi-directional radar system should be used for maximum detection volume and reduction of ground wave interference. This will also allow better characterization of energy and shower orientation. A configuration with a large obstruction between receiver and transmitter (such as a mountain or earth curvature), which assures direct transmission is reduced, is preferable. Lastly, a fairly powerful transmitter should be run at just over 50 MHz to avoid direct reflection and difficulties with geometric effects. This will also allow a relatively strong SNR in a remote location. Transmitting radar over the Telescope Array within these parameters should present an ideal system.

Bibliography

- [1] Greisen, K. End to the cosmic-ray spectrum? *Physical Review Letters*, 16(17): 748, 1966.
- [2] Kuz'min, V. A., and Zatsepin, G. T. Upper limit of the spectrum of cosmic rays. *Journal of Experimental and Theoretical Physics Letters*, 4:78, 1966.
- [3] Bird, D.J., et al. The cosmic-ray energy spectrum observed by the Fly's Eye. *Astrophysical Journal*, 424:491, 1994.
- [4] CERN Communication Group. Cern faq. <http://cdsmedia.cern.ch/img/CERN-Brochure-2008-001-Eng.pdf>, January 2008, Retrieved November 16th 10:34PM.
- [5] Gorham, P. W. On the possibility of radar detection of ultra-high energy cosmic ray- and neutrino-induced air showers. *Proceedings of the Royal Society of London. Series A. Mathematical and Physical Sciences*, 15:177, 2001.
- [6] Takai, H. On forward scattering extensive air shower bi-static radar. *Preprint submitted to Elsevier*, 2008.
- [7] Gorham, P. W. On radar detection of EeV air showers. *First International workshop on the radio detection of high energy particles, AIP Conference proceedings*, 579:253, 2001.

- [8] Terasawa, T., Nakamura, T., Sagawa, H., Miyamoto, H., Yoshida, H., Fukushima, M. Search for radio echoes from east with the mu radar, Shigaraki, Japan. *Proceedings of the 31st ICRC, LODZ*, 2009.
- [9] Yoshida, S. and Sigl, G. and Lee, S. . Extremely high energy neutrinos, neutrino hot dark matter, and the highest energy cosmic rays. *Physical Review Letters*, 81(25):5505, 1998.
- [10] Blakely, E. A. Biological effects of cosmic radiation: Deterministic and stochastic. *Health Physics: The Radiation Safety Journal*, 79:495, 2000.
- [11] Colwell, R. C., and Friend, A. W. The lower ionosphere. *Physical Review*, 50:632, 1936.
- [12] Watson Watt, R. A., Bainbridge-Bell, L. H., Wilkins, A. F., Bowen, E. G. Return of radio waves from the middle atmosphere. *Nature*, 137:866, 1936.
- [13] Watson Watt, R. A., Bainbridge-Bell, L. H., Wilkins, A. F., Bowen, E. G. The return of radio waves from the middle atmosphere. *Proceedings of the Royal Society of London. Series A. Mathematical and Physical Sciences*, 161:181, 1936.
- [14] Appleton, E. V., and Piddington, J. H. The reflexion coefficients of ionospheric regions. *Proceedings of the Royal Society of London. Series A. Mathematical and Physical Sciences*, 164:467, 1937.
- [15] Blackett, P.M.S., and Lovell, A.C.B. Radio echoes and cosmic ray showers. *Proceedings of the Royal Society of London. Series A. Mathematical and Physical Sciences*, 177:183, 1940.
- [16] Joseph J. Carr. *Practical Antenna Handbook Fourth Edition*. The McGraw Hill Companies Inc., 2001.

- [17] Vinogradova, T., Chapin, E., Gorham, P., Saltzberg, D. Proposed experiment to detect air showers with the jicamarca radar system. *First International workshop on the radio detection of high energy particles, AIP Conference proceedings*, 579: 271, 2001.
- [18] Kamata, K., and Nishimura, J. The lateral and the angular structure functions of electron showers. *Progress of Theoretical Physics Supplement*, 6:93, 1958.
- [19] Greisen, K. *Progress in Cosmic Ray Physics*, 3:Ed: Wilson, J.G. North Holland, 1965.
- [20] Matano, T., Nagano, M., Suga, K., Tanahashi, G. Tokyo large air shower project. *Canadian Journal of Physics*, 46:S255, 1968.
- [21] Vidmar, R.J. On the use of atmospheric pressure plasmas as electromagnetic reflectors and absorbers. *IEEE Transactions on Plasma Science*, 18(4):733, 1990.
- [22] Belz, J.W., Takai, H., Thompson, G. Project Proposal to the NSF. 2009.
- [23] KATHREIN-Werke KG. K52348. Directional Antenna 47...88 MHz. <http://www.kathrein.de//en/bca/products/download/936A753b.pdf>, 2009, Retrieved August 26th 3:24 PM.
- [24] LMNO Engineering. Static Pressure Calculation. <http://www.lmnoeng.com/Statics/pressure.htm>, Last updated 2001, Retrieved November 25th 4:41 AM.
- [25] Suprun, D.A., Gorham, P.W., Rosner, J.L. Synchrotron radiation at radio frequencies from cosmic ray air showers. *Astroparticle Physics*, 20(2):157, 2003.
- [26] Satellite Signals. Noise temperature, Noise Figure and Noise Factor. <http://www.satsig.net/noise.htm>, Last updated 25 March 2007, Retrieved November 25th 4:41 AM.

- [27] U.S. Navy Atmospheric Propagation Branch. AREPS Program. Last updated 03 September 2009, Retrieved November 25th 7:11 AM.

Appendix A

AREPS Instruction

The purpose of this appendix is to lead the reader through the process of reproducing the propagation attenuation graph for a transmitter and receiver system at the Telescope Array Project.

A.1 Installing the Program

The AREPS software is designed to run on a personal computer under Microsoft Windows 95, 98, NT 4.0, 2000, or XP operating systems. In a Linux operating system AREPS must be run in Wine.

- a) To start first *create an account at <http://areps.spawar.navy.mil/> by clicking **”Create AREPS account”***
- b) Once account information has been received *log in under **”My AREPS account”** with your account information. Then click the download link and install to the preferred directory.*
- c) Now that the AREPS software is installed and running *click on the **”Create a New Research Project”** icon on the second row of the start up screen to get started.*

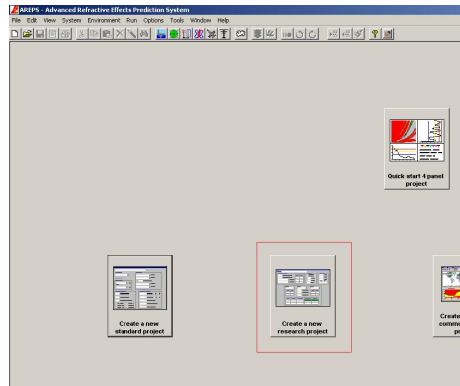


Figure A.1: Starting screen

A.2 Input EM System Parameters

- a) *Enter the project name in the "Project Label" area. I chose "TA Transmitter."*



Figure A.2: Project label

Next is the "EM system parameters" section.

- b) For "Frequency (MHz)" *enter the center operating frequency of the transmitter. The value for our current transmitter is 55.25Mhz.*
- c) The "Vertical beam width" is the vertical width of the antenna main beam. *Leave this at the default of 3 Degrees. This makes no visible difference on the end data at the range of the Telescope Array.*
- d) "Antenna elevation angle" is the direction of the maximum radiated power and is measured from the local horizontal and increases in an upward direction.

Pattern angle (Deg)	Pattern factor (Normalized)
-90	.05
-89	.052
-88	.053
-87	.055
-86	.058
-85	.06

Figure A.3: EM system parameters

For a perfectly vertical antenna enter 0 degrees.

- e) Next is "**Antenna height**" which is measured from ground level. *To reproduce the given graph enter 50 ft.*
- f) From the "**Polarization**" pull down menu *select the desired polarization.* The current estimated setup is horizontal polarization.
- g) Now for the "**Antenna type**" pull down *select "User defined"*
- h) *Right click the "Pattern angle" box and select "Pattern angle (Deg)" then right click the "Pattern factor" box and select "Pattern factor (Normalized)".*
- i) *Then right click the blank lines below the previous boxes and select "Read antenna pattern from file" and select the appropriate antenna pattern from their saved location.* If the polarization previously selected was horizontal then use the vertical pattern and vice versa.

The format of the antenna pattern file used must be a text file (.txt) with the following at the top:

AntennaType = "(put antenna type name here)"

AngleUnits = deg

FactorUnits = normalized

0 1.000

The first number is the angle and the second is the power factor for that angle. The angles specified must only be from 90 to -90 degrees and can be in any order.

A.3 Selecting the APM (Advanced Propagation Model) Properties

The next section is the APM (Advanced Propagation Model) area.

- a) *Check the "Include troposcatter" box and select "Full coverage mode."*

The other modes are not appropriate for accurate calculations directly above the Telescope Array.

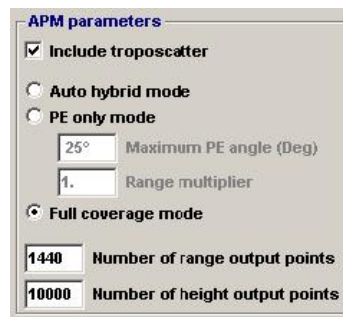


Figure A.4: APM parameters

- b) Below "Full coverage mode" are two boxes to input how many data points to calculate. *The recommend input values are the maximum number of range output points which is 1440 and the maximum number of height output points*

which is 10000. The maximum number does not take an inordinate amount of time on modern computers.

A.4 Selecting Environmental inputs

Now we'll look at the "Environmental inputs or files" section.

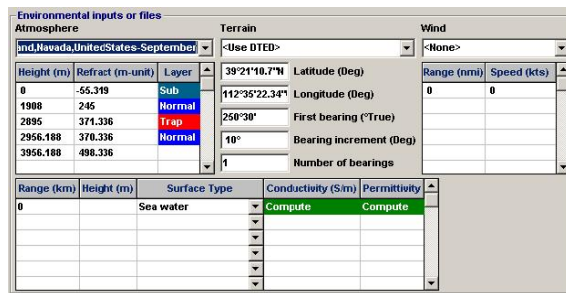


Figure A.5: Environmental inputs or files

- a) First is "Atmosphere". This section makes very little difference for general purposes. It is generally sufficient to *select* "<Standard>" from the drop down menu.

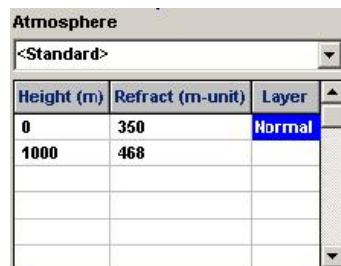



Figure A.6: Atmosphere

If a very high degree of accuracy is required an environment file will need to be created.

- b) To create an environment file *click on the*  *icon on the bar at the top.*
- c) In the new window that appears *select* **”Upper air Climatology.”** **”Surface Climatology”** is only data for the first few meters above ground.

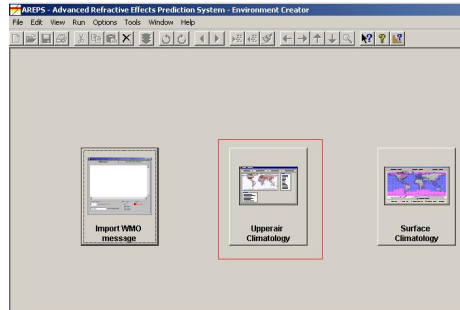


Figure A.7: Environment creator menu

- d) Next *select the month and* **”Ely/Yelland, Nevada, United States”** (which is the closest included data to TA). Then *save the environment file.*
- e) Now to use the environment file created *select the file from the drop down menu in the* **”Environmental inputs”** *section in the main AREPS program window.*

Next input data into the **”Terrain”** subsection.

- f) *Select* **”<Use DTED>”** *from the drop down menu.*
- g) Then *input the coordinates for the transmitter position in decimal form.* For a transmitter positioned at the Cosmic Ray Center(CRC) at 39°21’10.7”N 112° 35’22.34”W this is 39.352972 for **”Latitude (Deg)”** and -112.589538 for **”Longitude (Deg)”**.
- h) In the box titled **”Bearing increment (Deg)”** *input the number of degrees from north that will make an intersecting line from the transmitter to the receiver.* From the CRC to the Longridge site this is about 250.5 or 250°30’.

Terrain	
<Use DTED>	
39°21'10.7"N	Latitude (Deg)
112°35'22.34"W	Longitude (Deg)
250°30'	First bearing (True)
10°	Bearing increment (Deg)
1	Number of bearings

Figure A.8: Terrain

- i) The wind section can be ignored completely.

A.5 Input Display Options

Display options	
1400.	Minimum height (m)
3500.	Maximum height (m)
60.	Maximum range (km)
Propagation <input checked="" type="radio"/> loss <input type="radio"/> factor	
50.	Minimum loss (dB)
10.	Loss increment (dB)
12.	Number of increments

Figure A.9: Display options


Pictured above are the nominal settings for transmitting from the CRC to Longridge. 1400 meters is the elevation at the CRC. 3500 meters is just above X_{max} and 60 meters is just a bit farther than the distance from CRC to Longridge. To input the values in meters (and have meters displayed in the final product):

- a) *Select* "Options" > "Program Flow" from the menu bar.

- b) Under "Miscellaneous Defaults" select "Metric" for initialization units.
- c) Right click the display options area and select "Meters (m)"

Warning: When inputting 12 for the number of increments you will receive a warning that this setting is unstable. **This can be ignored.**

A.6 Generating the data

- a) When ready to generate the data click on  at the top bar. On the first run you will receive a pop up that looks something like the following:

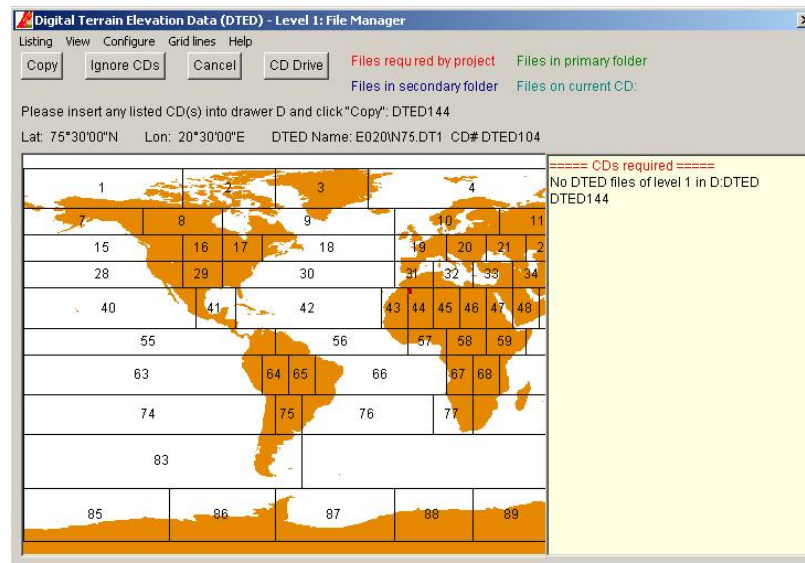


Figure A.10: Terrain Elevation Data File Manager

This is because the program needs the terrain data for the area being transmitted over.

- b) To find out what files are needed click on "Listing" > "# Files required for project" from the popup's menu bar. On the right hand side a listing will appear like this (the actual files will be different):

==== Files required ====

4 DTED files required for project.

W005\N28.DT1: Swap to CD: DTED144

W005\N29.DT1: Swap to CD: DTED144

W006\N28.DT1: Swap to CD: DTED144

W006\N29.DT1: Swap to CD: DTED144

- c) To download the indicated files *go to* <http://edcns17.cr.usgs.gov/EarthExplorer/> and create an account by clicking on **”Register”** at the top of the page.
- d) Under the **”Select your dataset(s)”** section *select* **”Digital Elevation”** and *check the box next to* **”SRTM”**.

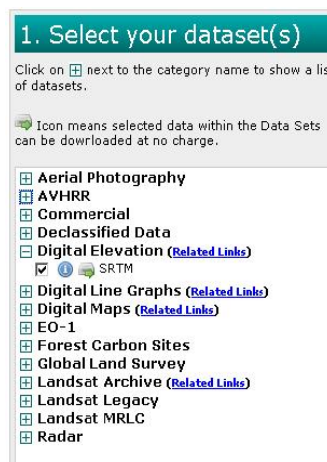




Figure A.11: Dataset selection

- e) In the **”Area Selected”** section *click the*  and *select one corner of the area on the Google map and then do the same for the opposite corner. Then click* **”Search”**.

Now that the search results are listed we’re interested in only **3-arc resolution files**. The **”Entity ID”** corresponds to the file name. The first example file needed **W005\N28.DT1** corresponds to an **”Entity ID”** of **SRTM3N28W005**.

- f) To download the example file *click on "SRTM3N28W005"* then *log in using your account information*.
- g) Then *download it into the AREPS directory ~/AREPS30/DATA/Dted/w005*. The last subdirectory corresponds to the end of the file name.
- h) When all of the required files have been saved *once again click on* . Then you will see something like pictured on the following page:

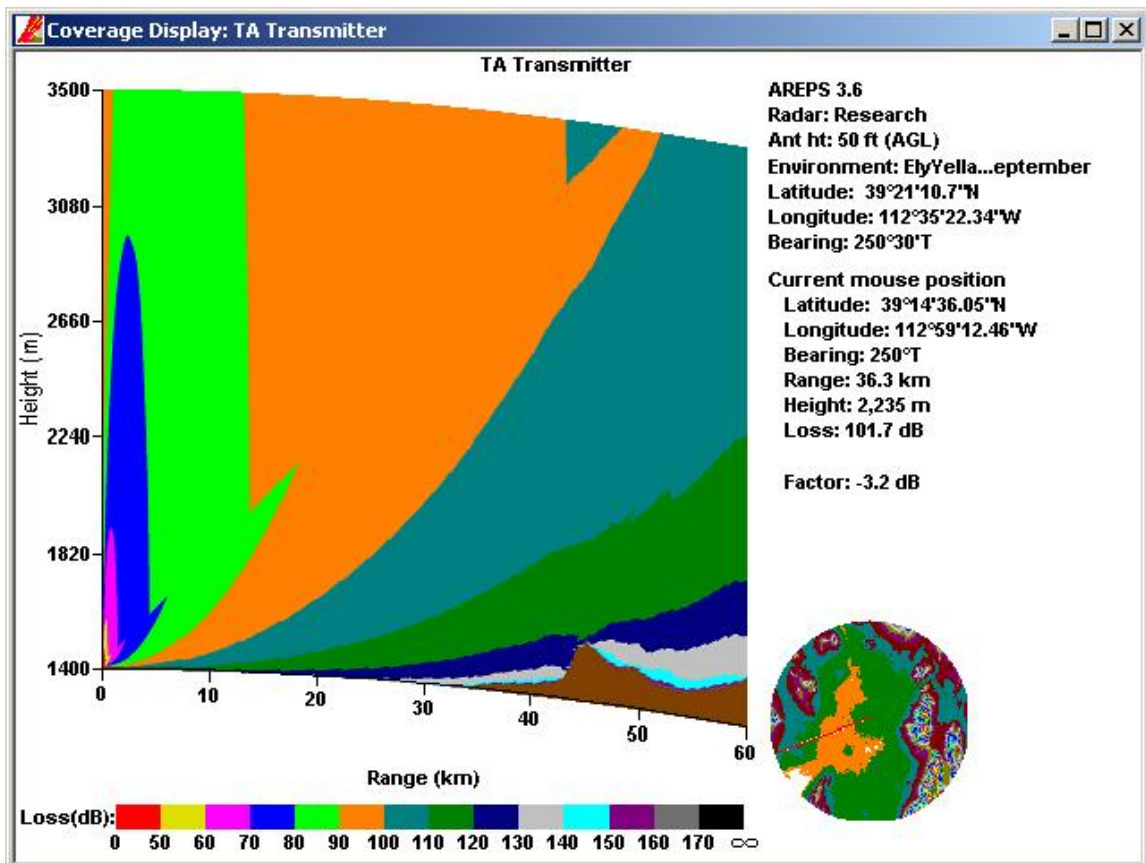


Figure A.12: The Final Product – Coverage Display

- i) If you would like to use the data points for other purposes *right click the graph and select "Save all APM data in ASCII text format"*.

Name of Candidate: Jon Paul Lundquist
Birth Date: 01 August 1980
Birth Place: Chicago, IL
Address: 180 C ST APT 9, Salt Lake City, UT